Thomson, D., and Bradley, R. (1998) The principles and practical application of helicopter inverse simulation. Simulation Theory and Practice, 6 (1). pp. 47-70. ISSN 0928-4869

The Principles and Practical Application of Helicopter Inverse Simulation

Dr Douglas G. Thomson
Department of Aerospace Engineering
University of Glasgow
Glasgow
G12 8QQ
Fax: 0141 330 5560
e-mail: d.g.thomson@aero.gla.ac.uk

Prof. Roy Bradley
Department of Mathematics
Glasgow Caledonian University
Cowcaddens Road
Glasgow
G4 0BA

Abbreviated Title:
Helicopter Inverse Simulation

Abstract

Inverse simulation is a technique whereby the control actions required for a modelled vehicle to fly a specified manoeuvre can be established. In this paper the general concepts of inverse simulation are introduced, and an algorithm designed specifically to achieve inverse simulation of a single main and tail rotor helicopter is presented. An important element of an inverse simulation is the design of the input functions i.e. manoeuvre definitions, and the methods used are also detailed. A helicopter mathematical model is also discussed along with the validation and verification of the inverse simulation. Finally, the applicability of the method is demonstrated by illustration of its use in two flight dynamics studies.

Keywords

Helicopter, Simulation, Modelling

Nomenclature

g	acceleration due to gravity	(m/s^2)
g_{TR}	tail rotor gearing ratio	
h	height of obstacle in hurdle-hop manoeuvre	(m)
I_R	inertia of main rotor	(kg m^2)
I_{tr}	effective inertia of transmission and gearing	(kg m^2)
I_{xx}, I_{yy}, I_{zz}	helicopter moments of inertia about centre of gravity	(kg m^2)
I_{xz}	helicopter product of inertia about y-axis	(kg m^2)
K_3	overall gain of engine/rotorspeed governor	(Nm/rad/s)
L, M, N	components of external moments on vehicle	(Nm)
m	helicopter mass	(kg)
p, q, r	components of helicopter angular velocity at centre of gravity	(rad/s)
Q_E	engine torque output	(Nm)
u, v, w	translational velocity components of helicopter centre of gravity	(m/s)
V_f	helicopter flight velocity	(m/s)
X, Y, Z	components of external force on vehicle	(N)
α	angle of incidence the fuselage	(rad)
β	main rotor blade flapping angle	(rad)
β	angle of sideslip the fuselage	(rad)
θ_0	main rotor collective pitch angle	(rad)
θ_{1_s}, θ_{1_c}	main rotor longitudinal and lateral cyclic pitch angles	(rad)
τ_{e1}, τ_{e2}, τ_{e3}	engine and rotorspeed governor time constants	(s)
ϕ, θ, ψ	body roll, pitch and sideslip attitude angles	(rad)
X	turn rate	(rad/s)
Ω	angular velocity of main rotor	(rad/s)
Ω_{idle}	angular velocity of main rotor at idle	(rad/s)
Ω_{TR}	angular velocity of tail rotor	(rad/s)

1. Introduction

The conventional approach to aircraft flight simulation is to develop a mathematical model of the subject vehicle and then compute its response to a set of piloting commands [12]. When the equations of motion of the mathematical model are solved in real-time then the computed response may be used to drive motion and visual systems. In this familiar application the simulation is widely used for training and vehicle evaluation. In practice, simulation models are more often used off-line (non real-time) to assess an aircraft's response to control stimuli or to examine its stability characteristics.

For a helicopter, such investigations, though valuable, do not represent an adequate coverage of the vehicle's operational activities. The crucial advantage of a helicopter is its ability to operate close to the ground tracking a precise flight path - something which is virtually impossible to replicate efficiently in an off-line simulation since the required control inputs are not known *a priori*.

Difficult problems often attract the advice to invert the problem - which in this case would be to supply the required flight path and recast the mathematical model so that it predicts the piloting commands required by the helicopter. This paper describes a method by which this may be done for a fully non-linear, flight mechanics model of a conventional helicopter. The complexity of the helicopter configuration guarantees that the inversion of such a model is significantly more difficult than for a fixed wing case. The method developed is in effect a discretisation of the nonlinear differential equations of motion, allowing subsequent numerical algebraic solution. It follows then that the method will be applicable to systems other than the helicopter provided the equations of motion are of the same form.

The sections 2 and 3 of this paper give brief introductions to helicopter flight and the general principle behind the inversion of the helicopter model. A feature of any inverse simulation is to provide the input to the simulation in an appropriate form. In the present case, a formal description of a helicopter manoeuvre is required. Although it is a relatively simple matter to give informal descriptions of typical manoeuvres, a precise, formal description requires a modelling strategy which can be validated in its own right. Section 4 sets out the modelling of some typical manoeuvres. A description of the helicopter mathematical model used in this study (HGS - Helicopter Generic Simulation) is presented in section 5. Next, the recasting of the mathematical model into a form suitable for inverse simulation is described and the resulting algorithm (Helinv - Helicopter Inverse Simulation) outlined. The form of the inverse simulation is a simple time-marching calculation which is both efficient and robust. A sample calculation using inverse simulation follows and then section 8 addresses the validation

of the flight path specifications and the inverse simulation. It is, of course, this vital validation step that gives credibility to the simulation's subsequent use.

Having developed a validated inverse simulation environment, the final section of the paper examines some studies which have practical application and shows the power and scope of this research tool. Within the overall development of the simulation and the discussion of some practical applications for the specific case of helicopter flight, several points of general relevance are discussed.

2. The Basic Principles of Helicopter Flight

There are two fundamental differences between helicopter flight and that of conventional fixed wing aircraft. Firstly the helicopter has the ability to fly at low speed and in the hover, and secondly, as a consequence of its low speed performance, the helicopter has the ability to follow precise trajectories and thereby manoeuvre close to obstacles such as trees, buildings and, of course, the ground. This added flexibility is at the expense of payload and operating cost - low speed flight implies less lift from the aerodynamic surfaces and hence lower payload for the helicopter. Given the radically different nature of the two aircraft it is perhaps no surprise that the method of flying them and the principles behind their operation are quite different. Although the principles and control of fixed wing aircraft flight may be familiar to many readers it is perhaps appropriate here to give some insight into these aspects of helicopter flight [4, 11].

The basic control method is by varying the magnitude and direction of the main rotor thrust vector. The magnitude of the thrust is controlled by collectively altering the pitch (and hence lift) of all of the rotor blades together by an means of the collective lever. This *collective pitch* displacement is denoted θ_0. As well as collective pitch control the pilot is also able to vary the pitch of individual blades cyclically around a complete revolution. When the pilot applies *longitudinal cyclic pitch*, denoted θ_{1_s}, by pushing the *cyclic stick* forward, the blade travelling towards rear of the disc flaps upwards, whilst the blade travelling towards the front of the disc flaps downwards. The net effect is that the thrust vector is tilted forward simultaneously pitching the vehicle's nose down allowing accelerated flight in this direction. Similarly pushing the cyclic stick to one side (i.e. applying *lateral cyclic pitch*, denoted θ_{1_c}) increases the pitch of the blades on the opposite side of the rotor (producing upwards flap) and decreasing it on the other (producing downwards flap) thereby producing a net thrust tilt in the direction of the stick motion. This can be used to produce sideways or banked flight. Finally, the torque transmitted by the engine to the main rotor is balanced by an opposing moment produced due to the offset of the tail rotor thrust from the centre of gravity. The tail rotor thrust

is controlled through pedal displacements which alter the pitch, denoted $\theta_{0_{tr}}$, of the blades and by varying this thrust (and hence "anti-torque" moment) it is possible to control the heading of the aircraft.

The coupling problems associated with helicopter control can be appreciated by considering the simple example of a pilot wishing to accelerate his aircraft without changing heading or altitude. The acceleration is achieved by application of forward longitudinal cyclic, θ_{1_s}, which tilts the rotor disc forward. One effect of this is that the component of the thrust vector which balances the weight of the aircraft has been reduced, and hence if altitude is to be maintained the magnitude of the thrust vector must be increased by application of collective pitch, θ_0. The increased pitch causes increased blade drag and in order to maintain rotorspeed, engine torque is also increased and hence a tail rotor collective pitch, $\theta_{0_{tr}}$, input is required to maintain heading. If unopposed the change in side force due to the change in tail rotor thrust will cause the helicopter to drift to the side. To overcome this an opposing input in lateral cyclic, θ_{1_c} is required. In practice, the pilot's workload is kept at acceptable levels by introducing control mixing (via mechanical linkages or the flight control system), and equipping the helicopter with a rotorspeed governor. This simple example where inputs to all four control channels are required to undertake a very basic manoeuvre demonstrates the complexity of the system being modelled - particularly so, when the example above has ignored the aerodynamic asymmetry of a helicopter in forward flight.

3. Inverse Simulation

The exercise of calculating a system's response to a particular sequence of control inputs is well known. It is conveniently expressed as the initial value problem:

$$\dot{\boldsymbol{x}} = \boldsymbol{f}(\boldsymbol{x},\boldsymbol{u}); \quad \boldsymbol{x}(0) = \boldsymbol{x}_0 \tag{1}$$

$$\boldsymbol{y} = \boldsymbol{g}(\boldsymbol{x}) \tag{2}$$

where $\boldsymbol{x}$ is the state vector of the system, $\boldsymbol{u}$ is the control vector and $\boldsymbol{y}$ is the output vector. Equation (1) is a statement of the mathematical model describing the time-evolution of the state vector in response to an imposed time history for the control vector $\boldsymbol{u}$. The output equation (2) is a statement of how the observed output vector $\boldsymbol{y}$ is obtained from the state vector. Inverse simulation is so called because a pre-determined output vector $\boldsymbol{y}$ is used to calculate the control time histories $\boldsymbol{u}$ required to produce $\boldsymbol{y}$. Consequently, equations (1) and (2) are used in an implicit manner. For helicopter flight the usual output is the helicopter's flight path and the controls are the pilot's stick and pedal movements so that for the inverse problem the flight path

becomes the input and the output to be generated is the pilot's control movements. Equations (1) and (2) may be recast in order to demonstrate the method by differentiating (2) to give:

$$\dot{\boldsymbol{y}} = \frac{d\boldsymbol{g}}{d\boldsymbol{x}}\dot{\boldsymbol{x}} = \frac{d\boldsymbol{g}}{d\boldsymbol{x}}\boldsymbol{f}(\boldsymbol{x},\boldsymbol{u}) \tag{3}$$

where use has been made of equation (2). In the simple case where (3) is invertible with respect to $\boldsymbol{u}$ it is possible to write:

$$\boldsymbol{u} = \boldsymbol{h}(\boldsymbol{x}, \dot{\boldsymbol{y}}) \tag{4}$$

and substituting in equation (1) gives:

$$\dot{\boldsymbol{x}} = \boldsymbol{f}(\boldsymbol{x}, \boldsymbol{h}(\boldsymbol{x}, \dot{\boldsymbol{y}})) = \boldsymbol{F}(\boldsymbol{x}, \dot{\boldsymbol{y}}) \tag{5}$$

shows that equations (4) and (5) are indeed a complete statement of the inverse problem with $\dot{\boldsymbol{y}}$ as the input vector and $\boldsymbol{u}$ as the output vector. Equation (5) is a system forced by the rate of change of the original output vector and, in the form shown, clarifies a number of aspects of the practical application of inverse simulation. First, the characteristic dynamics of the system described by equation (5) may be quite different to those of the original system described by equation (1). The constraints imposed by the direct application of equation (2) significantly modify the original stability properties. This effect has been explored in some depth for helicopter inverse simulation in Reference 14 and it is important that the inverse simulation practitioner is aware of this, quite general, phenomenon otherwise he can be misled by the unusual behaviour of perturbations in inverse simulation compared to that of conventional simulation. The second observation to be made is that in equation (5) it is the time rate of change, $\dot{\boldsymbol{y}}$, which forces the system, not $\boldsymbol{y}$, and, also, if equation (3) is not invertible with respect to $\boldsymbol{u}$ then further differentiations of equation (2) will be necessary to provide additional equations to support the inversion process. The consequence is that higher order derivatives of $\boldsymbol{y}$ may appear as the forcing terms in the inverse formulation. The appearance of higher order derivatives indicates that care must be taken to ensure the proper smoothness of the demanded output $\boldsymbol{y}$ otherwise, even if a control response $\boldsymbol{u}$ can be calculated, it is unlikely to be of practical value. This consideration does nothing more than reflect practical limitations on a physical system. For example, the occurrence of discontinuous velocities will produce unrealistic accelerations which, in turn, require physically unattainable forces and control displacements. Therefore the proper definition of the required output $\boldsymbol{y}$ is a primary consideration in inverse simulation. It is treated in detail in section 4, to follow, in advance of a discussion of the inverse algorithm itself.

4. Manoeuvre Modelling

The helicopter's primary function is to manoeuvre close to the ground. Consequently in the execution of the flying task the pilot is able to employ visual cues provided by the ground and follow a flight path largely determined by a tracking task. Therefore, the work at Glasgow has concentrated on manoeuvres that are defined in terms of motion specified relative to an Earth-fixed frame of reference. In these circumstances an appropriate output equation, in the form of equation (2) is:-

$$\begin{bmatrix} \dot{x}_e \\ \dot{y}_e \\ \dot{z}_e \\ \Psi_e \end{bmatrix} = \begin{bmatrix} \cos\theta\cos\psi & \sin\phi\sin\theta\cos\psi - \cos\phi\sin\psi & \cos\phi\sin\theta\cos\psi + \cos\phi\sin\psi & 0 \\ \cos\theta\sin\psi & \sin\phi\sin\theta\sin\psi + \cos\phi\cos\psi & \cos\phi\sin\theta\sin\psi - \cos\phi\cos\psi & 0 \\ -\sin\theta & \sin\phi\cos\theta & \cos\phi\cos\theta & 0 \\ 0 & 0 & 0 & 1 \end{bmatrix} \begin{bmatrix} u \\ v \\ w \\ \psi \end{bmatrix} \tag{6}$$

The first three components of this equation relate the velocity components of the helicopter's centre of mass in body axes (u, v, w) to the components of an Earth-fixed frame of reference ($\dot{x}_e$, $\dot{y}_e$, $\dot{z}_e$) via the Euler or attitude angles (ϕ, θ, ψ). The fourth equation expresses the heading angle ψ in terms of a prescribed function of time Ψ_e.

Given $\dot{x}_e$, $\dot{y}_e$, $\dot{z}_e$ and Ψ_e as functions of time, the four scalar equations represented by (6) are to be used to define the four control inputs needed to fly the manoeuvre. The task of manoeuvre description, therefore, is to find functions of time: $\dot{x}_e$, $\dot{y}_e$, $\dot{z}_e$ and Ψ_e which will give a realistic description of a given manoeuvre.

4.1 The Pop-up Manoeuvre

As an example of a relatively simple, but practical, manoeuvre consider a longitudinal manoeuvre where the flight path is in a vertical plane. The 'pop-up' manoeuvre is used to avoid an obstacle by a rapid change of altitude during straight and level flight (Figure 1).

Without loss of generality the manoeuvre is considered to take place in the (x_e, z_e) plane so that both the heading, Ψ_e, and lateral displacement, y_e, can be set to zero throughout. During the manoeuvre the altitude must change smoothly from its datum of zero to the height, h, needed to clear the obstacle. The co-ordinate z_e must therefore change smoothly from zero to $-h$ during the interval of time t_m needed to complete the manoeuvre. A smooth transition is accommodated by the polynomial function:

$$z_e(t) = -\left[6\left(\frac{t}{t_m}\right)^5 - 15\left(\frac{t}{t_m}\right)^4 + 10\left(\frac{t}{t_m}\right)^3\right]h; \qquad 0 < t < t_m \tag{7}$$

As discussed in the previous section, the fifth order polynomial for the altitude imparts a realistic degree of smoothness. The horizontal speed over the ground could also be specified directly but it has been found more convenient to specify the total flight speed V_f as a function of time (it is often constant) so that the horizontal component may be found from:

$$\dot{x}_e(t) = \sqrt{V_f(t)^2 - \dot{z}_e(t)^2}\,.$$

The manoeuvre time t_m is determined from the horizontal distance, s, to be covered during the pop-up:

$$s = \int_0^{t_m} \dot{x}_e(t)dt$$

which is easily solved by straightforward iteration.

The approach applied to the pop-up has wide applicability. Many manoeuvres take place in the vertical plane, and simply require appropriate polynomial, or piecewise polynomial functions to capture the essential characteristics of the manoeuvre. The main requirement is to ensure a sufficient degree of smoothness at the entry to and exit from any section of the manoeuvre. A similar approach can be applied to manoeuvres in horizontal plane. The Slalom, for example, is a 'S' shaped flight path flown at constant altitude and can be treated by the same principles.

As may be expected, a general flight path can also be described by specifying $\dot{x}_e$, $\dot{y}_e$, $\dot{z}_e$ and Ψ_e directly as functions of time following the principles discussed in the previous example. Often, however, the indirect specification of the flight path in terms of the secondary variables angle of climb, γ, and track angle, χ, is more natural. The situation is depicted in Figure 2 and the conversion to Earth axes is simply:

$$\begin{aligned}
\dot{x}_e(t) &= V_f(t)\cos\chi(t)\cos\gamma(t) \\
\dot{y}_e(t) &= V_f(t)\sin\chi(t)\cos\gamma(t) \\
\dot{z}_e(t) &= V_f(t)\sin\gamma(t)
\end{aligned} \qquad (8)$$

This form is particularly useful in turning flight - for example in the specification of banked turn to reverse the direction of flight and very good correlation between the modelled flight path and those derived from flight data has been observed [13]. In such manoeuvres, the specification of the heading angle, needed to complement the specification of the flight path co-ordinates to achieve a complete description of constraints, is usually inappropriate. Control of the angle of side-slip is often used by the pilot as part of the control strategy so the facility to

specify the side-slip angle as a function of time in included in Helinv. When this option is selected the final component of equation (6) is replaced by:

$$\beta(t) = \sin^{-1}\left(\frac{v}{V_f}\right)$$

where $\beta(t)$ is a predetermined function of time.

4.2 The Banked Turn Manoeuvre

As an example, consider the banked turn through an angle χ_e, Figure 3(a). Let the manoeuvre take place in the horizontal plane so that g is zero and for the purpose of this example let the flight velocity be constant (a smooth polynomial can be employed to vary the speed through the manoeuvre). The turn rate is the smooth pulse illustrated in Figure 3(b). There is a smooth entry to, and exit from, an interval of constant turn rate. The duration of the exit and entry transients are taken to be a chosen fraction of the total track angle, χ_e. From comparison with flight data [13] this fraction is pre-set as 0.15; as in previous work, the smooth transitions are described by polynomials of order 5. The unknown parameters, total time, t_m, and maximum turn rate χ_{max} in the description can be obtained by specifying an equivalent radius for the flight path and noting that the area beneath the turn rate curve must equal to the total angle χ_e.

These two examples serve to illustrate the general rules of manoeuvre design. The guiding principles are to use a simple basis for their description, and to use the most economic form consistent with smooth output from inverse simulation. The package, Helinv, incorporates several sets of pre-programmed, generic manoeuvre descriptions developed along the lines described above. The sets include Nap-of the Earth [13], Offshore Operations [16] and Mission Task Elements [3]. There is also a facility for bringing flight test data directly into the simulation environment.

5. A Description of the Helicopter Generic Simulation (HGS)

Given the complexity of the helicopter as discussed in section 2, it will be of no surprise that the simulation of these vehicles is a challenging problem. The focus in this paper is on the helicopter inverse simulation package, Helinv, and therefore in this section details are given of the helicopter model, HGS (Helicopter Generic Simulation) [15] used by Helinv. Although this model is firmly embedded within the helicopter inverse simulation, Helinv, the HGS mathematical model also exists independently of Helinv and can be used in a conventional manner. For the purpose of this paper a version of the model which has simplified rotor

dynamics will be discussed (i.e. only the fuselage and rotorspeed degrees of freedom are incorporated) so that the state vector is

$$x = [u\ v\ w\ p\ q\ r\ \phi\ \theta\ \psi\ \Omega\ Q_E]^T$$

where u, v, w are the components of translational velocity relative to a body fixed reference frame (x_b, y_b, z_b),

p, q, r are angular velocities about the body axes,

ϕ, θ, ψ are the Euler (or attitude) angles relating the body fixed axes set to the earth fixed inertial frame (x_e, y_e, z_e),

Ω is the angular velocity of the main rotor and

Q_E is the torque output of the engines.

Other, more comprehensive, models include the rotor blade flapping and lagging as states (individual blades have *lagging* motion in the plane of the "disc" to alleviate the hub moment due to aerodynamic drag and *flapping* motion out of the disc plane due to aerodynamic lift) and the dynamics of the rotor induced flow are also often included [4, 11]. In the version of the HGS model referred to in this paper these effects are assumed to occur instantaneously and the values of the states associated with these motions are obtained via intermediate calculations.

The control vector may be written as

$$u = [\theta_0\ \theta_{1_s}\ \theta_{1_c}\ \theta_{0_{tr}}]^T$$

where θ_0, θ_{1_s}, θ_{1_c}, and $\theta_{0_{tr}}$ represent main and tail rotor blade pitch angles.

Considering again equation (1), the function f consists, essentially, of the following equations. The fuselage degrees of freedom are described by the familiar Euler rigid body equations where because of the symmetry of the fuselage about the xz plane only the I_{xz} product of inertia is retained:

$$\dot{u} = -(wq - vr) + \frac{X}{m} - g\sin\theta \tag{9.1}$$

$$\dot{v} = -(ur - wp) + \frac{Y}{m} + g\cos\theta\sin\phi \tag{9.2}$$

$$\dot{w} = -(vp - uq) + \frac{Z}{m} + g\cos\theta\cos\phi \tag{9.3}$$

$$I_{xx}\dot{p} = (I_{yy} - I_{zz})qr + I_{xz}(\dot{r} + pq) + L \tag{9.4}$$

$$I_{yy}\dot{q} = (I_{zz} - I_{xx})rp + I_{xz}(r^2 - p^2) + M \tag{9.5}$$

$$I_{zz}\dot{r} = (I_{xx} - I_{yy})pq + I_{xz}(\dot{p} - qr) + N \tag{9.6}$$

where m, I_{xx}, I_{yy}, I_{zz}, and I_{xz} are the aircraft's mass, moments of inertia and product of inertia respectively. The symbols used for the vehicle states have their usual meaning as indicated in Figure 4. In order to get these equations of motion into the standard form of equation (1) it is necessary to eliminate $\dot{p}$ and $\dot{r}$ from the right hand sides of equations (9.4) and (9.6) to get:

$$\dot{p} = \frac{I_{zz}L^* + I_{xz}N^*}{I_{xx}I_{zz} - I_{xz}^2} \quad \text{and} \quad \dot{r} = \frac{I_{xx}N^* + I_{xz}L^*}{I_{xx}I_{zz} - I_{xz}^2}$$

where

$$L^* = (I_{yy} - I_{zz})qr + I_{xz}pq + L \quad \text{and} \quad N^* = (I_{xx} - I_{yy})pq - I_{xz}qr + N$$

The rate of change of the attitude angles are related to the body axes angular velocities by the kinematic expressions:

$$\dot{\phi} = p + q\sin\phi\tan\theta + r\cos\phi\tan\theta \tag{9.7}$$

$$\dot{\theta} = q\cos\phi - r\sin\phi \tag{9.8}$$

$$\dot{\psi} = q\sin\phi\sec\theta + r\cos\phi\sec\theta \tag{9.9}$$

Finally, the rotorspeed governor equations as given by Padfield [9] are

$$\ddot{Q}_E = \frac{1}{\tau_{e_1}\tau_{e_2}}\left[-\left(\tau_{e_1} + \tau_{e_3}\right)\dot{Q}_E - Q_E + K_3\left(\Omega - \Omega_{idle} + \tau_{e_2}\dot{\Omega}\right)\right] \tag{9.10}$$

$$\dot{\Omega} = (Q_E - Q_R - g_{TR}Q_{TR} - Q_{tr}) / I_R + \dot{r} \tag{9.11}$$

where τ_{e1}, τ_{e2}, τ_{e3}, K_3 are the time constants and gain of the governor,
Ω_{idle} is the angular velocity of the rotor in idle,
g_{TR} tail/main rotor gearing ratio,
Q_R, Q_{TR}, Q_{tr} are the torques required to drive the main rotor, tail rotor and transmission, and
I_R is the effective inertia of the rotor system.

Equations (9.1 - 9.9) are of course not unique to the helicopter, they are widely used in many rigid body simulations, and it is in the calculation of the external forces and moments X, Y, Z, L, M, N that the modelling of specific systems is required. To derive expressions for the

external force and moments individual components of the vehicle are considered - the fuselage (including fin and tailplane), the main rotor and the tail rotor. The external forces and moments on the fuselage are entirely due to the aerodynamic loading and are calculated from look-up tables of appropriate wind tunnel data. In the context of flight simulation this is generally accepted as the most effective solution as computational aerodynamic techniques tend to be "processor intensive" particularly for the complex flow field and fuselage shape of a helicopter. The look-up tables give force and moment coefficients as functions of the incidence angles α (angle of attack) and β (angle of sideslip) which are given by

$$\tan\alpha = \frac{w}{u} \quad \text{and} \quad \sin\beta = \frac{v}{V_f} \tag{10}$$

where $V_f = \sqrt{u^2 + v^2 + w^2}$ = the flight velocity of the aircraft, and are therefore functions of the state vector.

The external forces and moments from the main rotor are calculated by obtaining expressions for the aerodynamic loads on a blade element, then summing these along the span of the blade. The lift and drag of each element will be a function of :

i) the local airstream velocity - this is obtained from consideration of the velocity of the centre of gravity (u, v, w), the angular velocity of the aircraft (p, q, r), the position of the element relative to the c.g. (dependant on hub location, spanwise position and azimuthal location of blade), and the angular velocity of the blade element relative to the body fixed frame (a function of the angular velocity of the rotor Ω as well as the flapping velocity $\dot{\beta}$),

ii) the local angle of attack - as well as being dependant the local velocity, this is a function of the blade control angles θ_0 (constant for the full rotation), θ_{1_s} and θ_{1_c} (dependent on azimuthal position of blade), and the blade twist. (This is a function of radial position - rotor blades are usually twisted with leading edge down towards the tip of the blade where the highest velocities are experienced. This is to ensure more even distribution of the aerodynamic lift along the span thereby reducing the structural bending moment at the root).

For the HGS model this summation has been performed symbolically to produce a series of complex expressions for the external loads of the complete rotor disc which are, as is apparent from above, nonlinear functions of all of the state and control variables. A more sophisticated approach involves performing the summations numerically for each blade. This so called "individual blade model" is of course much more computationally intensive but is now found in wider use [5, 6].

Expressions for the tail rotor external forces and moments are obtained in a similar manner to that described for the main rotor.

This model can easily be used in the conventional manner, that is solving equations (1) for the response of the vehicle, $\boldsymbol{x}$, to some input function, $\boldsymbol{u}$. In the following section the recasting of these equations into a form suitable for inverse simulation is discussed. The derivation and use of such a helicopter inverse simulation, Helinv, is discussed in some detail in the following section.

6. The Helinv Inverse Simulation Technique

The procedure that has been used with some success to solve the inverse problem for helicopters is to apply a simple first order implicit scheme to (1) and write:

$$\frac{\boldsymbol{x}_n - \boldsymbol{x}_{n-1}}{\Delta t} = \boldsymbol{f}(\boldsymbol{x}_n, \boldsymbol{u}_n)$$

$$\boldsymbol{y}_n = \boldsymbol{g}(\boldsymbol{x}_n)$$

where Δt is the differentiation step. The procedure is, given $\boldsymbol{x}_{n-1}$ and knowing $\boldsymbol{y}_n$ solve these equations for $\boldsymbol{x}_n$ and $\boldsymbol{u}_n$ as the basis for a simple time-marching solution method. An acceptable method is to make an initial guess for the values of the unknown quantities and use a discrete form of the Newton Raphson iteration to give rapid convergence to values of the state vector and control vector at time increment n. For the current application, the state vector is

$$\boldsymbol{x} = [u\ v\ w\ p\ q\ r\ \phi\ \theta\ \psi\ \Omega\ Q_E\ ]^{\mathrm{T}}$$

and the control vector is

$$\boldsymbol{u}\ = [\theta_0\ \theta_{1_s}\ \theta_{1_c}\ \theta_{0_{tr}}]^{\mathrm{T}}$$

To solve for these fifteen quantities there are the eleven state equations: 9.1 - 9.11, and the four constraint equations arising from (6). These equations may be differenced as described above and solved to obtain values for the next time value in a time marching manner. The solution of the full non linear system of algebraic equations of order 15 can be avoided by sequencing the calculation procedure in an appropriate way. While it is not possible to generalise such manipulation, it is certainly valuable to examine the possibility of such economies in any application, since the practical value of Helinv has arisen from the rapid manner in which simulation results can be obtained. Efficient performance is very desirable in

a simulation tool which is to be used for exploratory research. The iterative procedure can be reduced to the solution of seven equations in seven unknowns. The seven unknowns are

$$\theta,\ \phi,\ \Omega,\ \theta_0,\ \theta_{1s},\ \theta_{1c},\ \theta_{0tr}$$

From initial estimates of these quantities at time point n the solution process continues by finding values for *u,v and w* from equation (6). Since the Earth fixed components and heading angle are all known ,the estimates for θ and ϕ enable the body axes components to be found. The kinematic relations 9.7-9.9 may be recast to give

$$p = \dot{\phi} - \dot{\psi}\sin\theta$$
$$q = \dot{\theta}\cos\phi + \dot{\psi}\cos\theta\sin\phi$$
$$r = \dot{\psi}\cos\phi\cos\theta - \dot{\theta}\sin\phi$$

and in this form p,q and r at time point n may be found from backward differencing the attitude angles. For example:

$$p_n = \frac{(\phi_n - \phi_{n-1}) - (\psi_n - \psi_{n-1})\sin\theta_n}{\Delta t}$$

The rate of change of the rotorspeed needed for equation (9.11) is similarly obtained by backward differencing:

$$\dot{\Omega}_n = \frac{\Omega_n - \Omega_{n-1}}{\Delta t}$$

and the value of Q_{E_n} follows. In this way we see that all of the information is now available to solve the differenced form of 9.1 - 9.6, 9.10 for the seven quantities θ, ϕ, Ω, θ_0, θ_{1s}, θ_{1c}, θ_{0tr} at time point n.

7. Sample Result from Helinv Inverse Simulation

The mathematical model described in section 5 has been implemented in a generic form such that any helicopter of the single main and tail rotor class can be simulated by specifying an appropriate set of configurational data. This is demonstrated by the following example of inverse simulations of two different helicopters: the Westland Lynx and Aerospatiale (Eurocopter) Puma flying an identical manoeuvre. The configurational data is as given by Padfield [9] whilst the manoeuvre is a Pop-up (as described above) performed at a constant velocity (V_f) of 80 knots, to clear an obstacle of height (h) of 25m, whilst the manoeuvre time

(t_m) is calculated to give a distance covered of 200m. Results for inverse simulations of the two configurations flying this manoeuvre are presented in Figure 5.

Although both aircraft have basically the same configuration (single, 4 bladed main rotors etc.), the basic design on the rotors are significantly different - thereby imparting different characteristics. The Lynx, in fact, has what is termed a "semi-rigid" rotor as it does not possess flapping hinges (the moment produced at the root being reacted by the structural stiffness of flexible root sections) whilst the Puma has a "fully articulated" (i.e. hinged) rotor. This gives the Lynx greater agility with faster rate response to control inputs and ultimately smaller cyclic control inputs to achieve a particular attitude displacement. This is evident from the plot of longitudinal cyclic (which produces the pitching moment and hence pitch attitude) where the displacements required by the Lynx are much smaller than those of the Puma. Note that as both aircraft are flying the same manoeuvre the kinematics of the task are the same and therefore so is the pitch attitude. The roll attitude and tail rotor collective are in the opposite sense to one another as the rotors rotate in opposite directions. The Puma is also a larger aircraft with a greater disc loading than the Lynx and so larger collective inputs are also required.

This example demonstrates one of the main advantages in using inverse simulation: having defined the operational task it is possible to simulate several vehicles or several variants of the same vehicle performing this task. As well as the results shown in Figure 5, it is also possible to obtain the power and torque required as well as many other parameters providing useful performance information.

8. Verification and Validation of the Helinv Algorithm

It is a fairly simple matter to assess qualitatively the accuracy of the results from inverse simulation - the control inputs and state responses calculated to fly specific manoeuvres can usually be explained in a convincing manner in the context of the likely response of the real aircraft. Of course, a more rigorous approach is required and in common with other simulations this is treated in two parts. Firstly it is important to verify that the algorithm is functioning correctly. This verification is achieved by applying the control inputs derived from the inverse simulation to the corresponding conventional simulation. For the Helinv algorithm verification is a simple process as the inherent model, HGS is also available in the form of a conventional flight mechanics simulation. The verification process then consists of obtaining the control time histories required to fly a predetermined flight path and using these to drive the conventional simulation. A comparison is then made between the flight path produced and the one initially used as input to the inverse simulation. Clearly, if the inverse simulation is

functioning correctly then the control inputs should produce the same flight path (irrespective of whether the helicopter model is valid or not). An example of this is shown in Figure 6 where the control inputs for the Lynx shown in Figure 5 have been applied to the HGS model to derive the flight path response. The two flight paths are shown in Figure 6. From the plot of altitude it is obvious that there is little difference between the two apart from a very slight deviation at the end of the manoeuvre. The plot of the track, which should be a straight line along the x-axis, shows a deviation of less than 5cm over the 200m distance. These and similar results provide sufficient evidence that the algorithm is functioning in the intended manner.

The question of the validity of the results is also important - if any meaningful information is to be derived then the mathematical model must replicate the actions of the real aircraft. Inverse simulation provides a useful technique for validating mathematical models. The conventional approach is to apply identical inputs to both the model and the system being simulated and then compare the two responses. Inverse simulation allows the actual system response to be used as an input to the model, the aim being to predict the control actions that were required to produce it. The actual and predicted control inputs may then be compared and the validity of the model established. It should be noted that all of the state responses are also calculated and are comparable with the actual system data. The main advantages of this approach are discussed in Reference 2.

An example of such a validation exercise is demonstrated in Figure 7. Data from flight trials of a Westland Lynx helicopter were supplied by the Defence Research Agency [10] which included time histories of all of the states and controls as well as ground based measurements of the helicopter's position. The positional co-ordinates and heading histories were used as inputs to Helinv, whilst the response histories are compared with those calculated by Helinv. The manoeuvre featured in Figure 7 is a "Quick-hop" which is a rapid longitudinal translation at constant height and heading, from a hover flight state over a specified distance (in this example 300ft) ending in a stabilised hover. The comparison between flight data and simulation shows that the correct trend is being predicted in all controls albeit with different absolute displacements in some variables (lateral cyclic and tail rotor for example). Other variable show good prediction qualitative and quantitative agreement - pitch attitude and collective for example. These and other results suggest that the model is of sufficient fidelity to be a useful tool for flight mechanics studies.

9. Applications of Helicopter Inverse Simulation

So far in this paper the theory of inverse simulation as applied to helicopter manoeuvring has been described. In this section some of the problems to which the inverse simulation Helinv, has been applied are discussed. The aim is to show the range of problems to which inverse simulation can contribute, often in a way which compliments conventional methods but in many cases it provides a unique methodology upon which to base an analysis.

9.1 Configurational Design and Performance

An inverse simulation can be considered as an "analytical flight test" that is a mission goal can be specified, and the simulated vehicle forced to fly it. As has been demonstrated, the basic output from the simulation is in the form of time histories of states and controls. Other information relating to the performance aspects of the helicopter such as torque and power are also calculated and recorded. In effect, the results may be considered as "analytical flight data" and indeed this data may be as extensive as that produced in actual flight trials. Given also a generic mathematical model (such as that employed by Helinv, HGS) it is possible to study the effect of varying key configurational parameters on the performance of the vehicle whilst undertaking its operational tasks.

This is clearly demonstrated via an example where the effect of increasing mass on a helicopter's performance whilst flying a routine task is examined. The subject helicopter is the Westland Lynx, and the baseline configuration is assumed to have a mass of 3500kg and that its centre of gravity is directly below the rotor hub. This is compared with the same aircraft carrying a load of 500kg internally which is assumed to have shifted the centre of gravity a distance of 15cm aft of the rotor hub. All other parameters in the HGS model are identical for both cases. The defined task for this demonstration is 180° change in direction to be initiated from a velocity of 120 knots. The performance criteria are that the manoeuvre should be completed in less than 10 seconds and that altitude should be maintained throughout. The manoeuvre is modelled in the manner described in section 4.1, where $\chi_e = 180°$, and setting t_m as 10s gives a turn radius of 155m, maximum turn rate, $\dot{\chi}_{max}$, as 23°/s and a maximum normal load factor of 2.75.

Having defined the helicopter configurations and specified the manoeuvre, it is possible to perform inverse simulations of these configurations flying it. The control time histories generated are shown in Figure 8, from which the overall control strategy can be deduced. The manoeuvre is initiated by a pulse in lateral cyclic to roll the aircraft, note that there is little difference in the amount required between the two configurations. As the aircraft rolls, as shown in Figure 9, collective (and hence thrust) must be added to maintain altitude. There is

also a forward motion of the longitudinal stick (denoted by negative longitudinal cyclic) to maintain constant forward speed. The manoeuvre is performed without sideslip and tail rotor collective is used to ensure that this condition is met. The initial pulse in lateral cyclic is opposed by a similar pulse in tail rotor collective which then increases beyond its level flight trim position to offset the extra torque produced by increased main rotor collective. The main differences between the time histories of the two aircraft lie in the collective and longitudinal plots. The baseline configuration requires less collective firstly because it is lighter, but one must also consider the effect of shifting the centre of gravity aft of the rotor hub. This produces a nose up pitching moment which must be countered by forward stick if velocity is to be maintained, which explains the 4.5 degrees of extra forward longitudinal cyclic required by the loaded configuration. The longitudinal tilt of the thrust vector is in addition to the lateral tilt required for rolling, and hence is a contributory factory in the 2.5 degrees of extra collective required by the heavy configuration. Examination of Figure 9 shows that the roll angle history which was suggested by the manoeuvre definition is obtained, and the maximum bank angle reached was approximately 70 degrees, with roll rates of approximately 70 degrees/second encountered in the transients.

The advantage of this method becomes apparent when it is realised that the collective limit of this configuration is known to be 20 degrees. Consequently on examination of the collective time history in Figure 9 it is clear that the loaded configuration is close to the limiting case for this manoeuvre. It then follows that the limiting case for various aircraft masses and centre of gravity positions could be obtained by repeated inverse simulation of the manoeuvre thereby allowing the aircraft configuration envelope for this task to be derived. This process could, of course, be extended to include a whole series of tasks representing the operational envelope of the vehicle.

9.2 Assessment of Handling Qualities and Workload

The need to assess the overall handling qualities of a helicopter by its performance and handling characteristics in a range of typical manoeuvres has been recognised by the authors of the U.S. Handling Qualities for Military Rotorcraft [1]. As part of demonstrating compliance with these requirements, a set of standard manoeuvres, or Mission Task Elements (MTEs) has been defined and criteria for performance and handling have been specified. In addition, the authors of this document have indicated that mathematical models are an appropriate basis for evaluation and analysis at the design stage. By its nature, inverse simulation encapsulates this combination of precisely defined manoeuvre and mathematical modelling. As with the performance studies described above it may then be argued that the data obtained by inverse simulation can be processed and analysed in the same manner as that collected from flight trials, and equivalent handling qualities information for the modelled helicopter derived.

For example, consider a helicopter performing a Rapid Side-step MTE (a lateral translation from the hover accelerating to some maximum sidewards velocity, V_{max}, followed by a deceleration back to the hover). A mathematical description of this MTE is most conveniently achieved by assuming an acceleration profile as shown in Figure 10. In practice the maximum acceleration, $\dot{V}_{max}$, is specified along with the time to achieve it from a hover, t_a, and the time required to reach maximum deceleration, t_d. The value t_1 is then calculated such that the area under the acceleration phase of the profile is equal to the user specified maximum velocity, V_{max}. Taking this mathematical model and using it in conjunction with the inverse simulation results such as those in Figure 11 are obtained (where $\dot{V}_{max}$ = 5m/s^2, t_a = 1.5s, t_d = 3s and V_{max} = 35knots).

In the context of a flight trial, using data such as this it is possible to calculate values for the "Roll Quickness" parameter for each excursion in roll. This parameter is defined as the peak roll rate divided by the minimum roll attitude displacement during the excursion. When plotted against the roll displacement, this parameter gives an indication of the handling qualities of the vehicle in terms of Levels 1 -3 of the Handling Qualities Criteria [1]. In this case the modelled helicopter is again based on a Westland Lynx, and, as indicated in Figure 11, it is then possible to calculate values for the Roll Quickness parameter. As this exercise is easily repeatable for Rapid Side-steps of differing severity, it is possible to create a chart such as that shown in Figure 12 which predicts handling qualities for the Rapid Side-step in the Level1/Level 2 regions.

In fact, further studies have shown that parameters such as the roll quickness are primarily kinematic and are therefore more related to the task than to the helicopter [3]. In order to quantify those aspects of handling that are related to the pilot's control activity it is necessary to explore alternative parameters. Since inverse simulation predicts the control displacements needed to fly a manoeuvre it is ideally suited to studies of this kind.

10. Conclusions

This paper has described how the need to predict the pilot's control movements and the vehicle response for a helicopter flying a specified task has led to the development of a method for inverse simulation. The structure of the solution algorithm has been discussed in some detail since an efficient solution procedure is essential if the method is to be used as an exploratory research tool. Several applications in performance studies and handling qualities analysis have been described. From the point of view of the user, the value of helicopter inverse simulation is that attention is focused upon the practical tasks expected of the pilot and

the helicopter, and that the helicopter can be driven through severe manoeuvres in a manner that is achievable by no other technique.

These benefits are, in principle, applicable to a wide range of controlled dynamic systems. In section 3, the general principles of inverse simulation have been set out in a manner which may be readily adapted to systems other than helicopters. Some comments have been included which apply to the general situation. First, it is essential to define outputs which have a smoothness that is consistent with the dynamics of the constrained system. The degree of smoothness required may be discovered by analysis [3] or by experiment. For example, in the helicopter application described, the acceleration profile needs to have at least smooth second order derivatives in order to predict realistically smooth control movements by the pilot. Second, it is necessary to appreciate that the dynamics of the constrained system may be quite different from the unconstrained. The properties of the internal dynamics, that is, those not constrained by fixing the output, are important to the success of inverse simulation. It should be realised that the internal dynamics are not an artefact of inverse simulation, they are the consequence of imposing a specific output to be followed. If the result is an unstable system then inverse simulation will correctly reflect that property.

In this paper the usefulness of inverse simulation as a tool in helicopter flight dynamics has been highlighted. The methodology presented is far from being specific to this application, indeed any dynamic system represented by a set of equations of motion may be treated in the same way. Hence whenever very precise forms of output are required from a system, there are substantial benefits to be gained during the research and development by inverting the system simulation.

Finally, the impact of inverse simulation in conveying real understanding of the systems under investigation should not be underestimated. For example, a fly-off of two competing helicopters through identical manoeuvres gives comparative information on pilot workload, handling qualities, and helicopter performance - and consequently gets right to the heart of practical flight dynamics requirements.

References

[1] Anon, Aeronautical Design Standard, Handling Qualities Requirements for Military Rotorcraft., ADS-33D, (1994).

[2] Bradley, R., Padfield, G.D., Murray-Smith, D.J., Thomson, D.G., Validation of Helicopter Mathematical Models, *Transactions of the Institute of Measurement and Control*, **12** (4) (1990) 186-196.

[3] Bradley, R., Thomson, D.G., The Development and Potential of Inverse Simulation for the Quantitative Assessment of Helicopter Handling Qualities, *Proceedings of the NASA/AHS Conference 'Piloting Vertical Flight Aircraft: Flying Qualities and Human Factors'*, San Francisco, USA (1993) 3.59-3.71.

[4] Bramwell, A.R.S., Helicopter Dynamics, (Arnold, London, 1976).

[5] Houston, S.S., Rotorcraft Simulation for Design Applications, *Proceedings of the 1992 European Simulation Multiconference*, (1992).

[6] McVicar, J.S.G., Bradley, R., A Generic Tilt-rotor Simulation Model with Parallel Implementation and Partial Periodic Trim Algorithm, *Proceedings of the 18th European Rotorcraft Forum*, Avignon, France (1992) 138.1-138.19.

[9] Padfield, G.D., A Theoretical Model of Helicopter Flight Mechanics for Application to Piloted Simulation, Royal Aircraft Establishment, TR 81048, (1981).

[10] Padfield, G.D., Charlton, M.T., Aspects of RAE Flight Research into Helicopter Agility and Pilot Control Strategy, *Proceedings of the Helicopter Handling Qualities Specialists Meeting*, Ames Research Center, Moffet Field, USA (1986).

[11] Padfield, G.D., Helicopter Flight Dynamics : The Theory and Application of Flying Qualities and Simulation Modelling, (Blackwell Science, Cambridge, 1995).

[12] Rolfe, J.M., Staples, K.J., Flight Simulation, (Cambridge University Press, Cambridge, 1989).

[13] Thomson, D.G., Bradley, R., Modelling and Classification of Helicopter Combat Manoeuvres, *Proceedings of the 17th ICAS Congress*, Stockholm, Sweden, (1990) 1763-1773.

[14] Thomson, D.G., Bradley, R., Prediction of the Dynamic Characteristics of helicopters in Constrained Flight, *The Aeronautical Journal*, **94** (940), (1990) 344-354

[15] Thomson, D.G., Development of a Generic Helicopter Model for Application to Inverse Simulation, University of Glasgow, Department of Aerospace Engineering, Internal Report No. 9216, (1992).

[16] Thomson, D.G., Talbot, N., Taylor, C., Bradley, R., Ablett, R., An Investigation of Piloting Strategies for Engine Failures During Take-off from Offshore Platforms, *The Aeronautical Journal*, **99** (981), (1995) 15-25

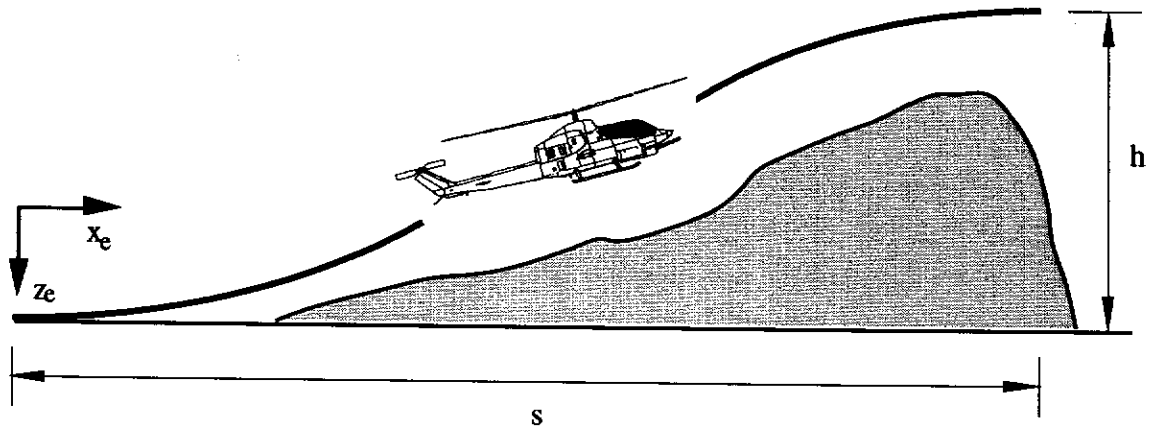

Figure 1 : The Pop-up Manoeuvre

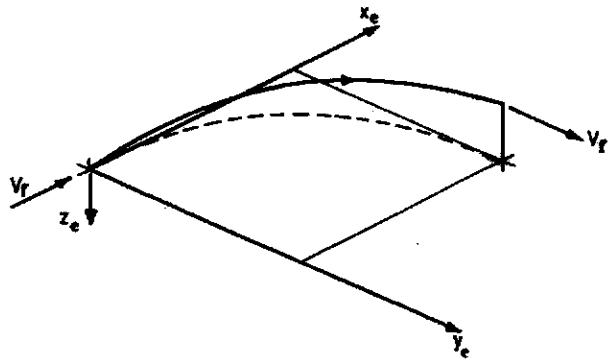

(a) A General 3-Dimensional Manoeuvre

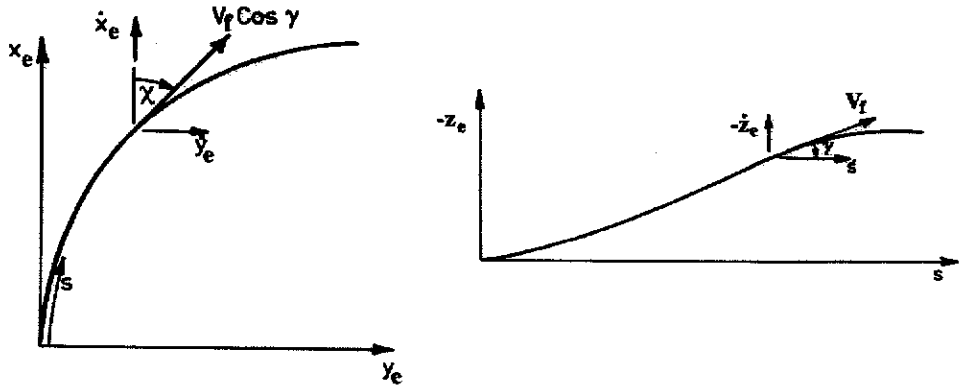

(b) The Track **(c) Altitude**

Figure 2 : General Definition of a Manoeuvre

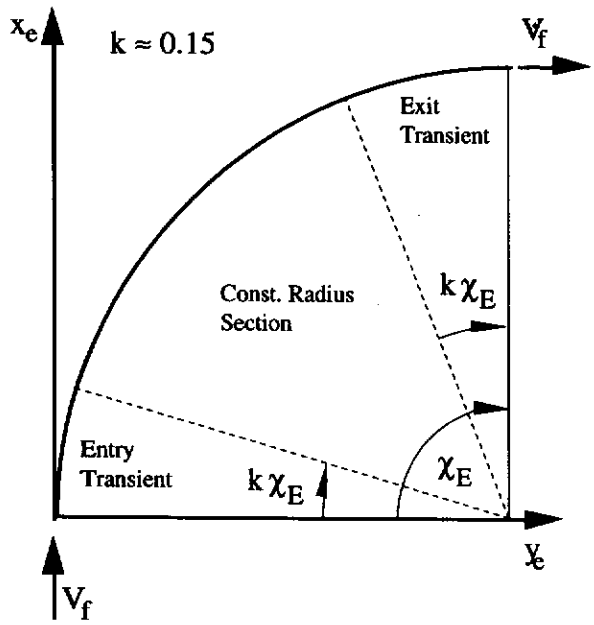

a) Aircraft Track

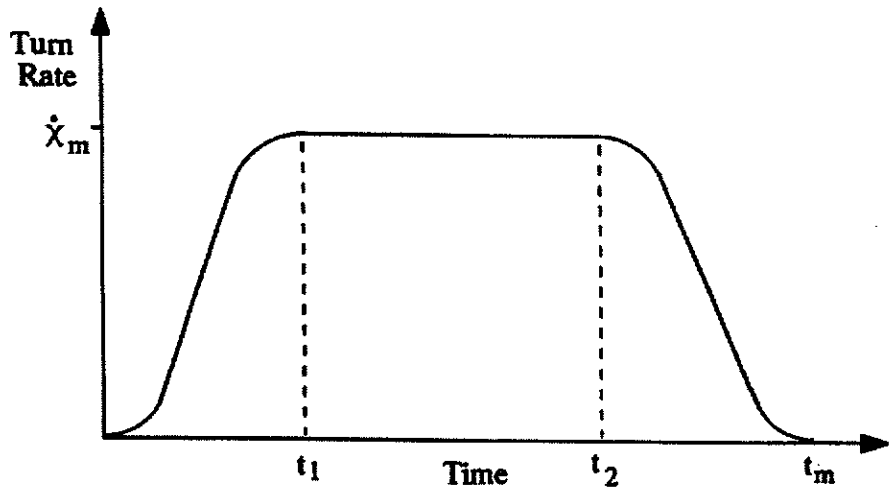

b) Turn Rate Profile

Figure 3: The Banked Turn Manoeuvre

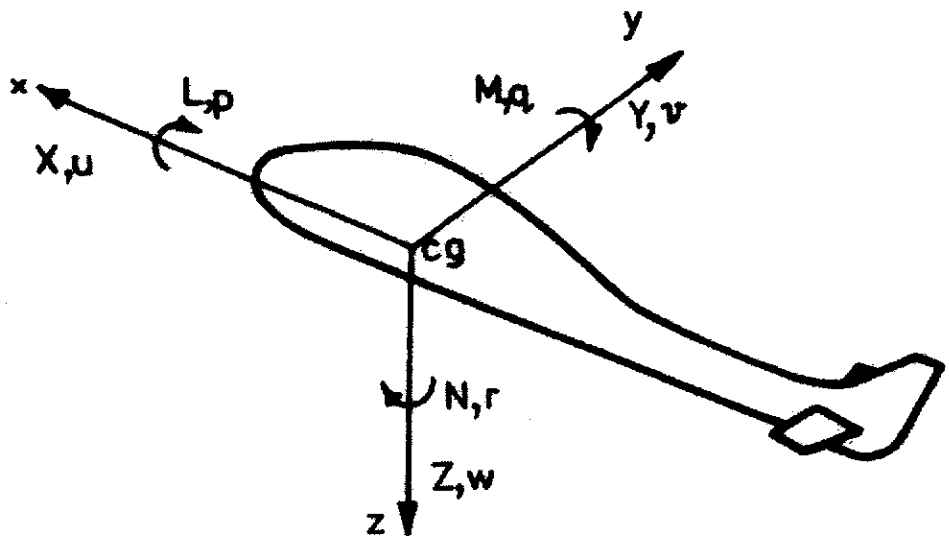

Figure 4 : The Body Fixed Reference Frame

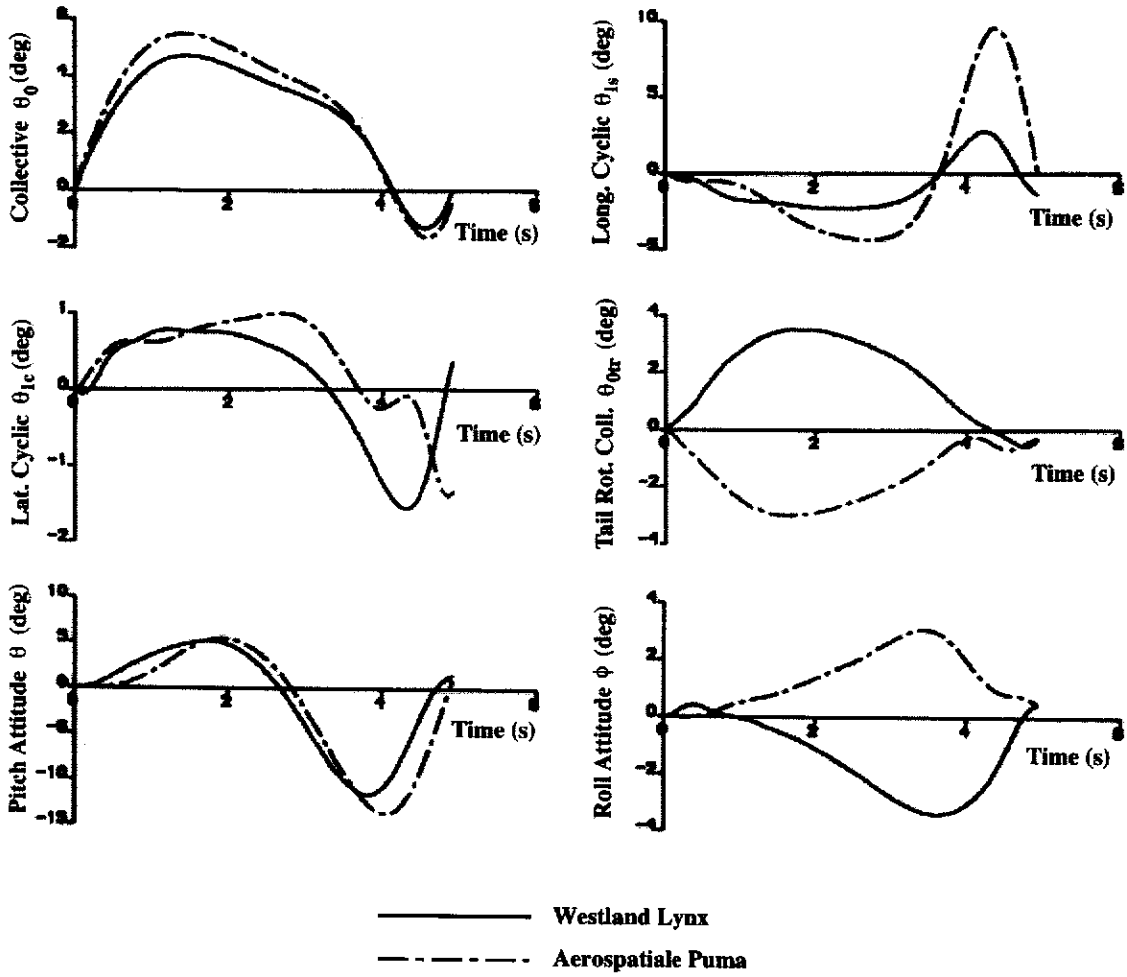

Figure 5 : Inverse Simulation Results for 2 Configurations Flying a Pop-up Manoeuvre

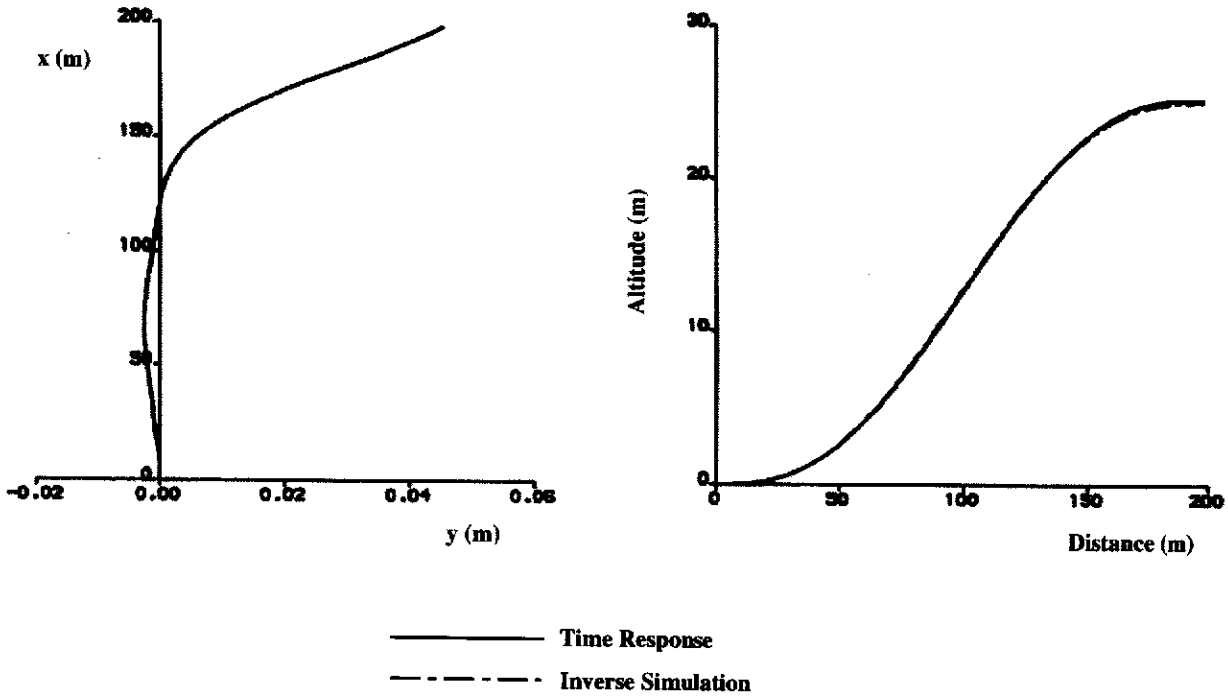

Figure 6 : Comparison of Flight Paths - Original Defined Path vs. Path Generated by Time Response Driven by Calculated Controls

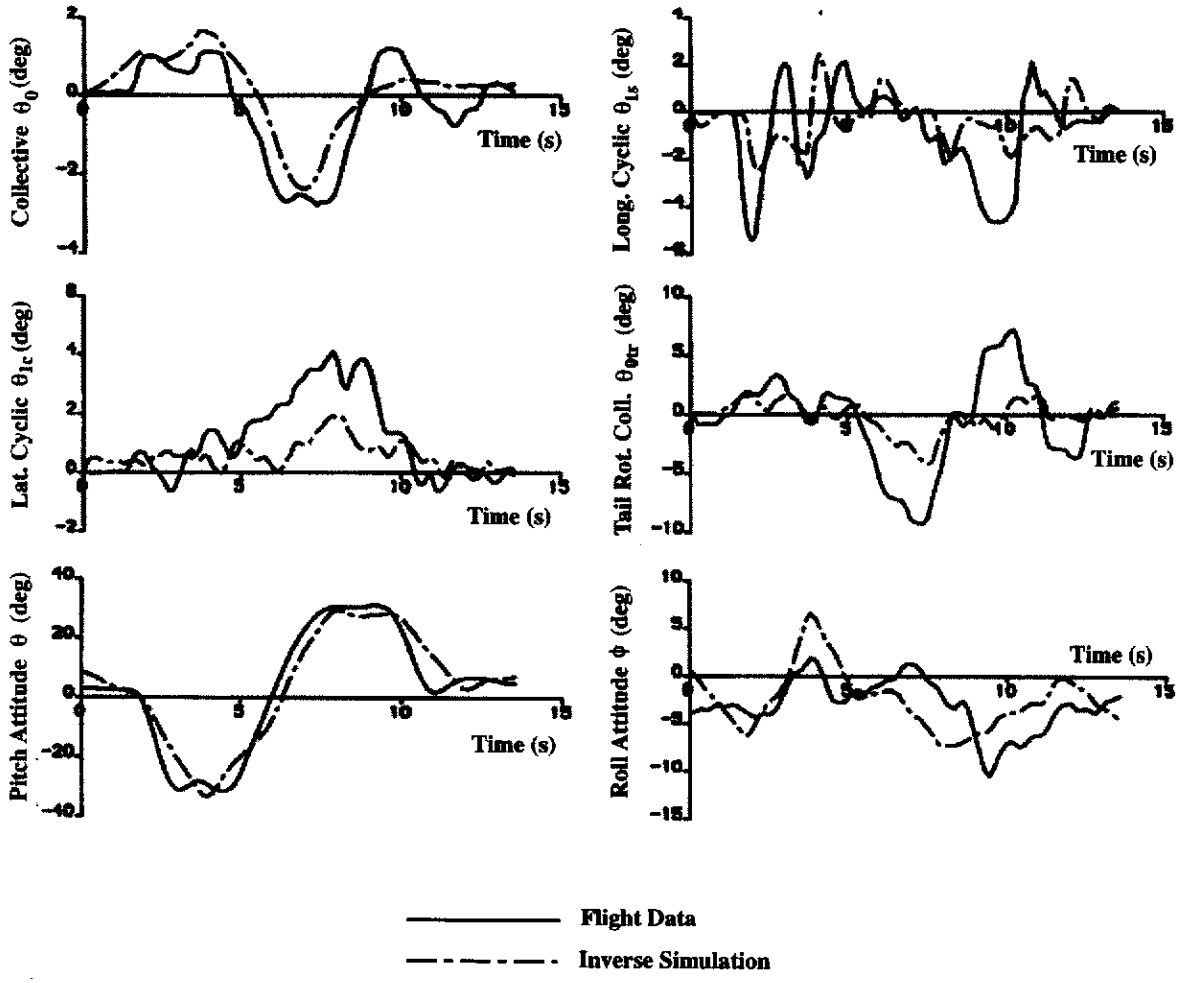

Figure 7 : Comparison of Flight Data and Inverse Simulation Results for a "Quick-hop" Manoeuvre

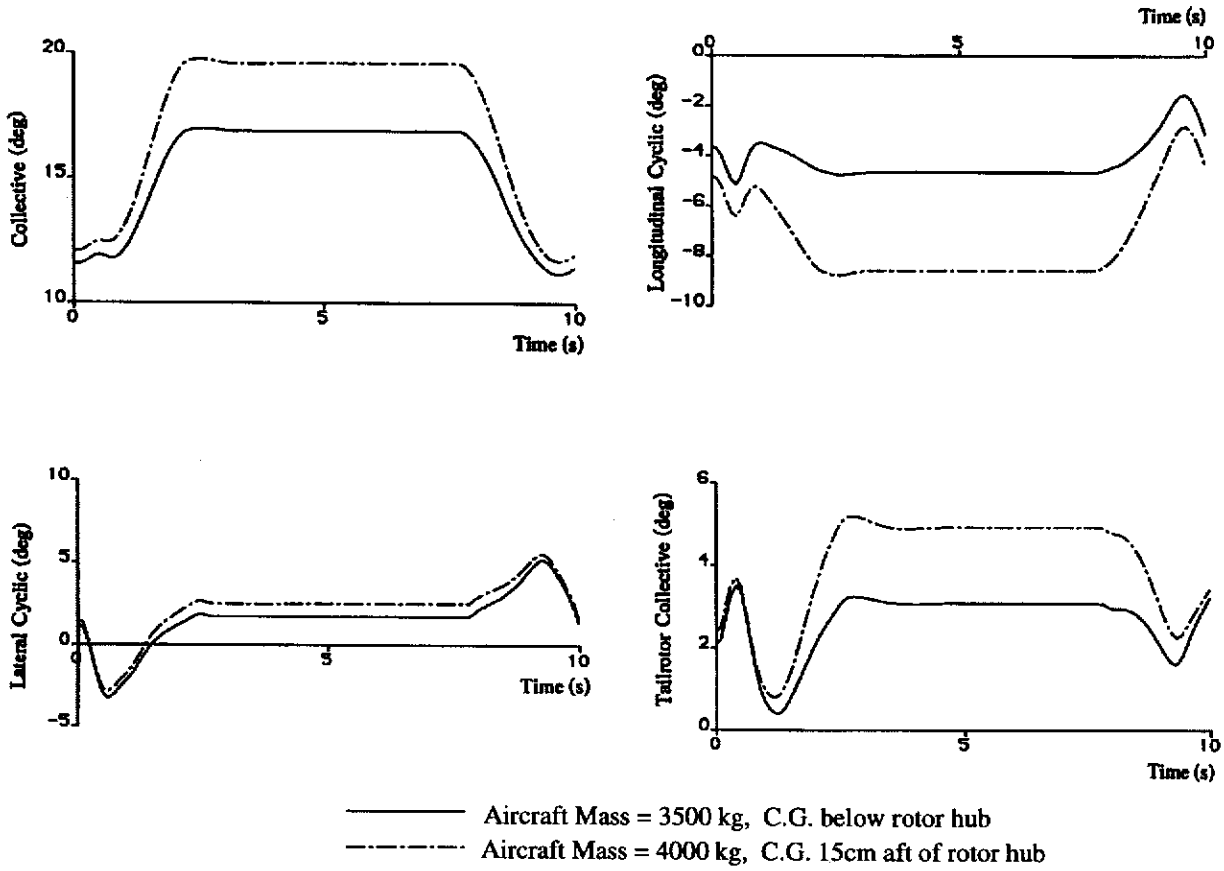

Figure 8 : Control Displacements Calculated by Inverse Simulation of a Lynx Flying a Banked Turn Manoeuvre

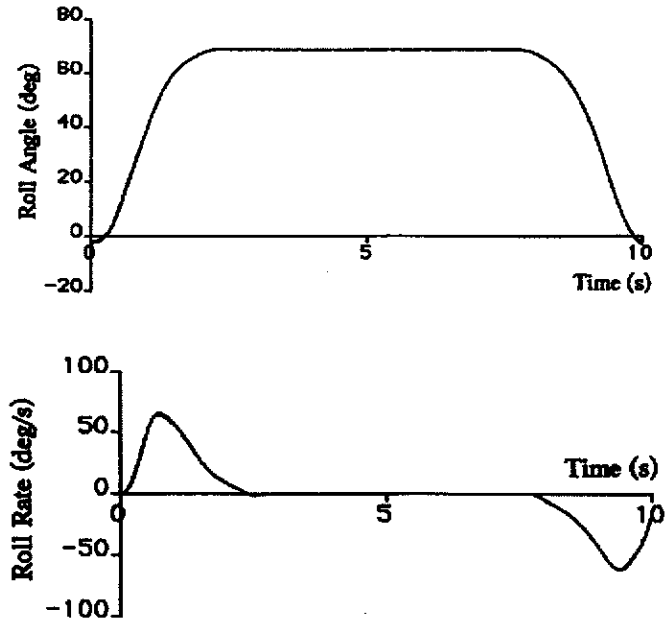

Figure 9 : Roll Angle and Rate From Inverse Simulation of Lynx Flying a Banked Turn Manoeuvre

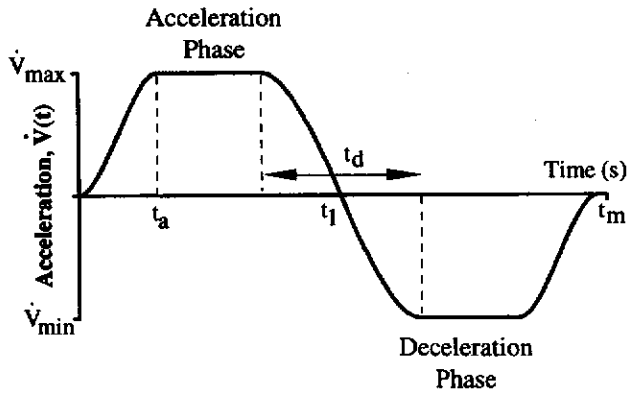

Figure 10 : Acceleration Profile for Rapid Side-step MTE

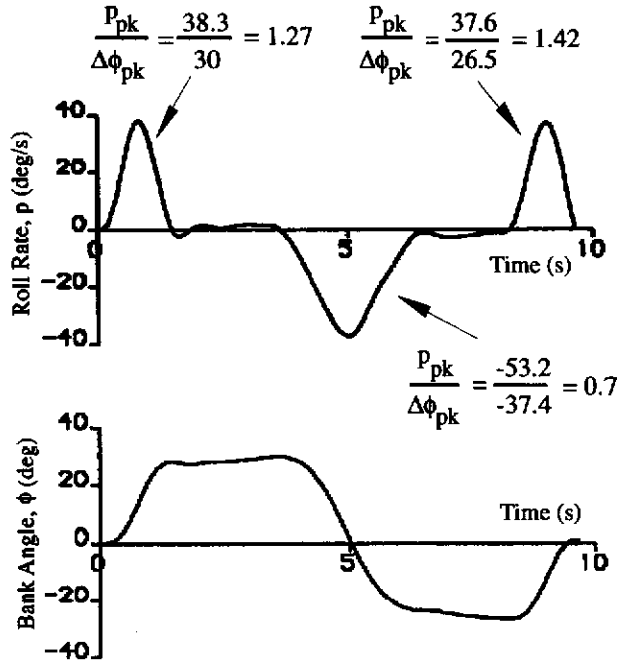

Figure 11 : Inverse Simulation Results for a Rapid Side-step MTE

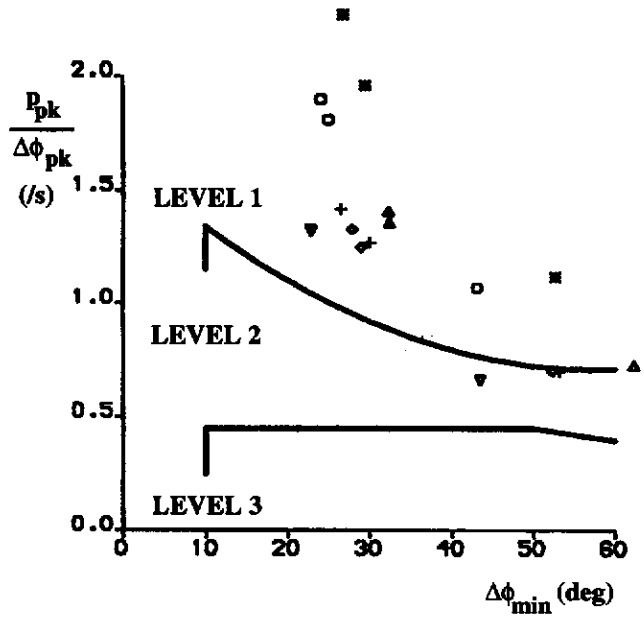

▲ V_{max} = 35 knots, t_a=1.5s, t_d = 3.0s, $\dot{V}_{max/min}$= ± 6m/s^2
✦ V_{max} = 35 knots, t_a=1.5s, t_d = 3.0s, $\dot{V}_{max/min}$= ± 5m/s^2
▼ V_{max} = 35 knots, t_a=1.5s, t_d = 3.0s, $\dot{V}_{max/min}$= ± 4m/s^2
◆ V_{max} = 50 knots, t_a=1.5s, t_d = 3.0s, $\dot{V}_{max/min}$= ± 6m/s^2
○ V_{max} = 35 knots, t_a=1.0s, t_d = 2.0s, $\dot{V}_{max/min}$= ± 4m/s^2
■ V_{max} = 35 knots, t_a=1.0s, t_d = 2.0s, $\dot{V}_{max/min}$= ± 5m/s^2

Figure 12 : Roll Attitude Quickness for Lynx Flying Rapid Side-step MTE